Analysis of the delocalized Raman modes of conformationally disordered polypeptides

L. X.-Q. Chen, H. L. Strauss, and R. G. Snyder
Department of Chemistry, University of California, Berkeley, California 94720 USA

ABSTRACT Bands associated with delocalized vibrational modes were identified in the isotropic Raman spectra of a series of polyglycine oligomers in aqueous solution as zwitterions and as cations. The dependence of these bands on conformational disorder and chain length was determined. The observed dependence is closely mimicked in spectra calculated for a series of corresponding model polypeptides. The simulated spectra were calculated in a skeletal approximation for ensembles of conformationally disordered chains. As the chain length of the conformationally disordered polypeptides increases, the observed isotropic spectra rapidly approach the spectrum of the infinitely long disordered chain. Convergence is nearly complete at the tripeptide for both the zwitterion and the cation. The simulated spectra behave in essentially the same way. Convergence to the spectrum of the infinitely long chain is much more rapid for the conformationally disordered polyglycines than for the ordered polyglycines because of the mode localization that results from disorder. In the low-frequency region the bands in the calculated spectra have frequencies that are systematically dependent on chain length. These bands are related to the longitudinal acoustic modes of the ordered chain.

INTRODUCTION

During the past few decades, through a combination of experiment and theory, extensive correlations have been established between vibrational frequencies and the structure of peptides and proteins, thus providing a basis for the determination of their complex structures (1–8). However, these earlier studies have focused mainly on structures that are static, whereas in fact most biological reactions occur in solution, where these molecules, being to some extent flexible, may have multiple conformers. Consequently, the focus of structural determination by vibrational spectroscopy has changed toward the characterization of the distribution of conformers and their dynamics. One approach to the spectroscopic identification of conformation is through the determination of the relation between vibrational frequencies and the bond rotation angles that define conformation (9–12). This involves the determination of a transferable vibrational force field. However, a reliable, transferable force field for peptides has not yet been determined. There are a number of reasons for this, foremost among them being the difficulty in evaluating with any kind of accuracy the very large number of independent force constants associated with these complex and structurally varied molecules. On the other hand, impressive advances have been made using molecular dynamics to simulate the large amplitude modes of macromolecules. This analysis allows us to visualize some of these low-frequency vibrations and to identify and characterize those motions that are directly associated with the biological function of the macromolecule (13, 14).

This work departs from earlier approaches to understanding the spectra of conformationally disordered peptide chains in that it attempts a more general characterization of the vibrations, concentrating on the effect of disorder on the localization of vibrational modes and how the disorder is reflected in the Raman spectrum of the peptide chains in solution. The effects of multiple conformers and chain length are also considered. To aid in exploring these relations, we have calculated the spectra of disordered model peptides. The structures of the model peptides have been greatly simplified, partly to simplify the calculation, but more importantly to eliminate a large number of vibrational modes that tend to obscure the characterizations we seek to establish.

Our approach to the problem is similar to what we have used to analyze the isotropic Raman spectra of assemblies of conformationally disordered *n*-alkanes (15–19). In these earlier analyses we characterized the vibrations in terms of their degree of spatial localization and in terms of the sensitivity of the frequencies and widths of the bands to chain length, average conformation, and internal rotation amplitude. The *n*-alkane study was greatly facilitated by the facts that the observed isotropic Raman spectra of these chains in the liquid state can be accurately simulated and that the normal coordinates that are required can be easily obtained from a well-established force field (20).

In this study as well as in our previous studies, we have focused on the isotropic component of the Raman spectrum rather than on the anisotropic component, both because the isotropic component is simpler to compute and to interpret (21–23) and because this spectrum contains significantly more information relating to chain conformation and skeletal mode delocalization. Isotropic intensities are easier to compute since the intensity parameters involved, namely, the mean polarizability derivatives, are scalar quantities. In addition, since bond stretching is normally by far the largest contributor, a good estimate of the observed isotropic spectrum can be obtained by considering only bond stretching, for which

Address correspondence to R. G. Snyder.
L. X.-Q. Chen's present address is Chemistry Division, Argonne National Laboratory, Argonne, IL 60439.

only one parameter per type of bond is needed. Because of the dominance of bond stretching, the isotropic spectrum is sensitive to conformation and reflects mode delocalization. The anisotropic Raman spectrum, on the other hand, is intrinsically much more complex. This spectrum is made up of contributions, not only from the stretching modes, but also from bending and torsional modes of all sorts. Their contributions enter into the calculations of the spectrum in the form of tensors, so that the simulation of the anisotropic spectrum is much more difficult than for the isotropic. Finally, we note that the bands in the anisotropic spectrum, just as in the infrared spectrum but not in the isotropic Raman spectrum, are significantly broadened by reorientational motion, which overlaps and obscures the effects of conformational disorder.

We report here some results of applying this approach to skeletal peptide chains. The peptide spectra, which were calculated under assumptions similar to those used in the *n*-alkane analysis, were used to establish the dependence of the calculated spectra on factors such as the degree of conformational disorder and the chain length. This dependence is compared with that found for the measured spectra of a series of polyglycyl peptides in aqueous solution.

First we describe our methods, both experimental and theoretical, and then discuss the isotropic Raman spectra of a homologous series of glycyl peptides, in both their zwitterion and cation forms. We note that the spectra change with increasing chain length and that certain bands are especially sensitive to conformation. A limited discussion of band assignments is included. In conclusion, we describe the calculated spectra and compare them with the spectra actually observed for the polyglycyl chains.

MATERIALS AND METHODS

Measurement of isotropic Raman spectra

Isotropic Raman spectra of glycine oligomer solutions were measured with a Raman spectrometer (model 1403; Spex Industries Inc., Meluchen, NJ) at a resolution of 4 cm^{-1}. Excitation was provided by the 514.5-Å line of an Ar^+ laser at a power of ~300 MW. A polarizer was placed after the sample for the measurement of parallel ($I_{||}$) and perpendicular ($I_{\perp}$) spectra. A polarization scrambler was used to eliminate polarization effects of the monochromator. Interference from the spectrum of water was a problem because the Raman intensities of the peptides in the dilute solutions are low. Therefore, solvent spectra were measured under the same conditions and subtracted from the solution spectra. Isotropic spectra were obtained by subtracting the perpendicular spectrum ($I_{\perp}$) from the weighted parallel spectrum ($\rho I_{||}$). The weighting factor ρ was empirically adjusted so that the depolarized component was eliminated. Its value ranged from 0.5 to 0.7.

The samples measured were aqueous solutions of polyglycines, G_n. The zwitterion form of the G_n have the formula $H_3N^+CH_2[CONHCH_2]_{n-1}COO^-$. For the cation, the COO^- group is replaced by COOH. All the polyglycines were purchased from Sigma Chemical Co. (St. Louis, MO) and used without further purification. The zwitterion form is present in the aqueous solution. Doubly distilled water was used to obtain the cations in solutions acidified with HCl. The isotropic Raman spectra of zwitterion solutions of samples G_n with n = 1–4 and of cation solutions with n = 3–5 were measured.

TABLE 1 Minimum potential energy conformations of *N*-acetyl-*N'*-methylglycinamide (from reference 24)

Conformation	ΔE*	Dihedral angles ϕ	Dihedral angles ψ
	kcal/mol		
1	1.240	180°	180°
2	0.000	79°	−73°
3	0.000	−79°	73°
4	1.217	73°	34°
5	1.217	−73°	−34°
6	1.438	167°	−52°
7	1.438	−167°	52°

* $\Delta E = E - E_0$, where E_0 is the lowest energy minimum.

Computational methods

We calculated the density of states, isotropic Raman spectra, and scattering activities of model peptides of structure $CH_3CONH—(CH_2CONH)_{n-1}—CH_3$. Since the aliphatic H atoms were not explicitly included in the computational model, their masses were incorporated into the carbon atoms of the CH_3 or CH_2 groups. Each —CONH— unit was assumed to be planar. The conformation of each peptide unit is determined by the pair of dihedral angles, ϕ, ψ, that flank the CH_2 group. We have used the conformational energy differences and dihedral angles defining conformation that were obtained by Vasquez et al. (24) for the peptide $CH_3—CONH—CH_2—CONH—CH_3$, using the program ECEPP (Empirical Conformational Energy Program for Peptides) described in reference 24. The minimum-energy conformational energies, and the seven pairs of values of ϕ and ψ that correspond to these minimum-energy conformational states, are listed in Table 1.

The isotropic Raman spectra of the conformationally ordered chains were calculated with $\phi = \psi = 180°$. The spectra of disordered assemblies of chains were simulated by summing the spectra of many randomly disordered chains. To define a conformer, one of the seven possible rotational conformations defined by discrete ϕ, ψ pairs was selected randomly to define conformation about each connecting methylene group. The values of the Boltzmann weighting factors for the conformers of the model peptide are based on the calculated energies. In calculating the frequencies and normal coordinates of each conformer, only the diagonal elements of the force constant matrix were used. The diagonal force constants were assigned values that give vibrational frequencies and potential energy distributions close to those that we obtained in more accurate calculations in which interaction force constants are included.

A bond polarizability model was used to calculate Raman intensities. Earlier studies have shown that bond stretching is by far the largest contributor to the isotropic intensity (21–23). Therefore, only bond stretching contributions have been included in the expression for the intensity I_k for the kth normal mode. We then have

$$I_k \propto \left(\sum_i^{str} L_{ik} \bar{\alpha}_i' \right)^2 B_k^{-1}, \quad (1)$$

where i refers to bond stretching coordinates, L_{ik} is an eigenvector element, and $\bar{\alpha}_i'$ is the mean polarizability derivative with respect to bond stretching. B_k, which is a Boltzmann factor that expresses the

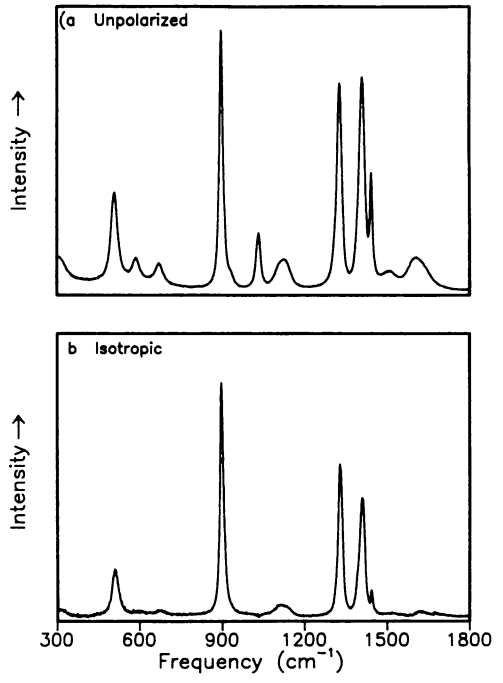

FIGURE 1 Raman spectra of glycine (G_1) zwitterions in aqueous solution at room temperature. (*a*) Unpolarized; (*b*) isotropic.

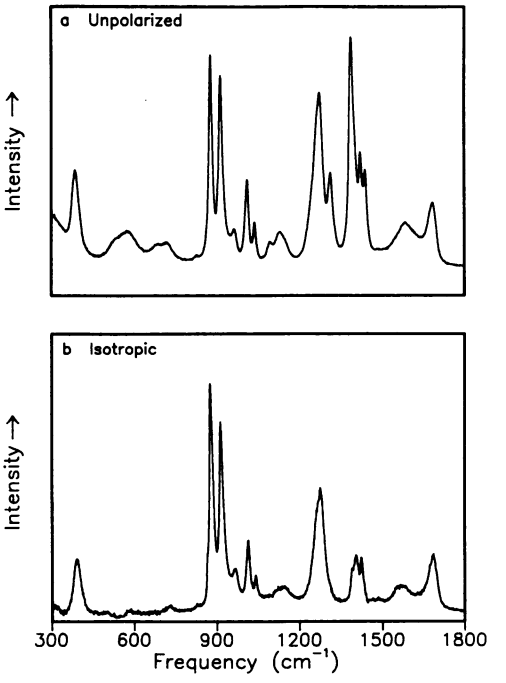

FIGURE 2 Raman spectra of glycylglycine (G_2) zwitterions in aqueous solution at room temperature. (*a*) Unpolarized; (*b*) isotropic.

temperature and frequency dependence of the Raman spectrum, is given by

$$B_k = \nu_k[1 - \exp(h\nu_k/RT)], \qquad (2)$$

where ν_k is the frequency of the mode and T is the temperature of the sample.

The spectrum used to compare with the observed spectrum was obtained by dividing the frequency region of interest into equal intervals of width $\Delta\nu$, the intervals being numbered $m = 1, 2, \ldots$, and by summing the total Raman intensity in each interval m

$$I_m = \sum_{r,k'} W_r I_k^{(r)}, \qquad (3)$$

where r designates a particular conformer, W_r is its weighting factor for conformer r based on its potential energy, and $I_k^{(r)}$ is the intensity of the k' mode of the conformer, included only if $\nu_{k'}$ lies in the frequency interval $\nu_m \pm \Delta\nu/2$. A spectrum was obtained by placing a Lorentzian band of intensity I_m at the center of each frequency interval. The full bandwidth at half maximum was assumed to be 8 cm^{-1} for all bands.

OBSERVED ISOTROPIC RAMAN SPECTRA GLYCYL PEPTIDES

Isotropic Raman spectra of the zwitterions

In this section we discuss the following for the zwitterions: the assignments of some bands; the differences between the unpolarized spectrum and the isotropic spectrum; and changes in the isotropic spectra related to changes in chain length. Figs. 1–4 show the observed Raman spectra, both unpolarized and isotropic, of glycine peptide zwitterion solutions at room temperature. These peptides consist of from one to four amino acids.

In Table 2 are listed some general assignments for bands in those frequency regions specifically of interest here. We note that there are unsettled differences in some of the assignments reported in the literature (9–11). With a few exceptions, we have not attempted to sort these out.

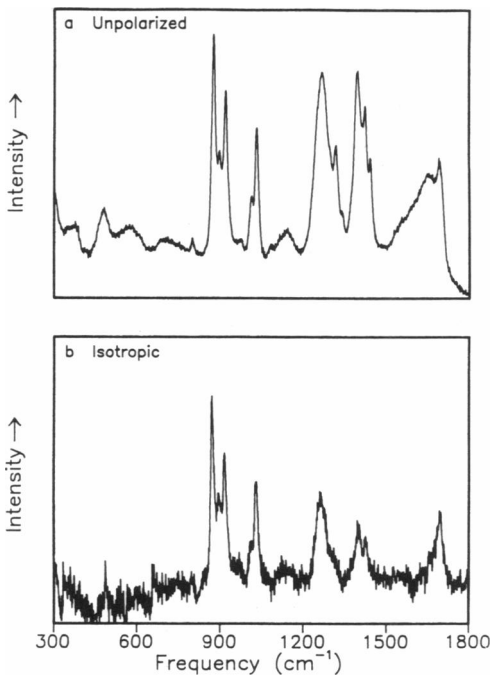

FIGURE 3 Raman spectra of glycylglycylglycine (G_3) zwitterions in aqueous solution at room temperature: (*a*) Unpolarized; (*b*) isotropic.

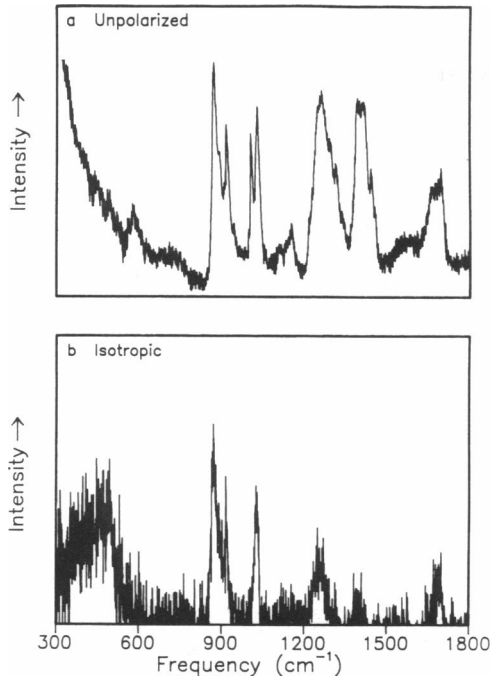

FIGURE 4 Raman spectra of glycylglycylglycylglycine (G_4) zwitterions in aqueous solution at room temperature: (*a*) Unpolarized; (*b*) isotropic.

The principal difference between the unpolarized and the isotropic Raman spectra is that some bands in the unpolarized spectrum do not appear in the isotropic spectra. These can be assumed to be associated with bending or possibly torsional modes, since these kinds of modes derive nearly all their intensity from the anisotropic component of the derivative of the polarizability tensor. As noted earlier, the intensity of isotropic bands is associated with the mean-polarizability derivative, to which bond stretching is the main contributor, bond angle deformation or internal rotation making only a minor contribution. The most intense isotropic band is the C=O stretching mode (amide I).

First we consider some assignments of bands in the light of our polarization measurements. For G_1 (Fig. 1), the four anisotropic bands near 1,448, 1,032, 659, and 577 cm^{-1} are probably bending modes because they are intense in the anisotropic Raman spectrum and weak at best in the isotropic spectrum. Thus, the earlier assignment (in reference 11) of the 1,448-cm^{-1} band to CH_2 scissoring is confirmed, but not the assignment of the 1,027-cm^{-1} band to C—N stretching. The anisotropic character of the bands near 577 and 659 cm^{-1} supports their assignment to —COO bending and torsion, respectively, as given earlier in references 10 and 11.

For the G_2 oligomer (Fig. 2), the bands at 1,395, 1,318, 1,098, 722, 684, 564, and 526 cm^{-1} are all anisotropic. This fact supports the earlier assignment of the bands at 1,395 and 1,318 cm^{-1} to wagging and bending modes of CH_2 and NH_3 groups as well as the assignment of bands in the 500–700-cm^{-1} region to out-of-plane bending and torsional modes (10, 11).

The isotropic Raman spectra of G_3 and G_4 (Figs. 3 and 4) are of poorer quality than those of G_1 and G_2. This is the case because, due to the low solubility of G_3 and G_4, the spectrum of the solvent overlaps that of the sample, and it is necessary to subtract it out. This subtraction, in addition to that necessary to obtain the isotropic spectra, results in a significant decrease in the signal-to-noise relative to that for the shorter chains. (Although some of the underside of the G_4 spectrum is missing in Fig. 4, the relevant spectral features are in evidence.)

In the low-frequency isotropic Raman spectra of the peptide solutions, there should appear a number of low-frequency bands that are associated with delocalized modes, similar to those that appear in this same frequency region for the liquid *n*-alkanes. These bands, which are conformationally sensitive, are related to the longitudinal acoustic modes (LAM) of the ordered chain (15, 16). The isotropic Raman spectrum of G_1 shows one such band at 510 cm^{-1}; the corresponding band for G_2 is at 382 cm^{-1}. The large downward frequency shift that is observed here in going from G_1 to G_2 suggests that this band represents a LAM-1–like mode. For each oligomer, there should be at least one intense isotropic band associated with LAM-1. The fact that there are no intense isotropic bands in the frequency region 600–300 cm^{-1} for $n > 2$ is easily explained since an extrapolation of the downward frequency shift observed for this band in going from $n = 1$ to $n = 2$ indicates that this band would have a frequency < 300 cm^{-1}. Thus, for chains longer than $n = 2$, this band would be beyond the frequency limit of our Raman measurements. At frequencies lower than ~300 cm^{-1}, the isotropic spectrum is obscured by intense anisotropic scattering from the sample. As chain length increases, the pattern of the bands in the isotropic Raman spectra of the glycyl peptide solutions tends to simplify and to converge asymptotically toward the spectrum of the infinitely long disordered chain. The convergence is quite rapid with increasing chain length. Consequently, the

TABLE 2 Approximate description of peptide vibrations according to frequency region

Frequency region	Approximate description*
cm^{-1}	
1,750–1,630	Amide I (C=O s)
1,550–1,500	Amide II (C—N s, NH ib)
1,470–1,400	CH_2 b, NH ib
1,380–1,310	CH_2 w, NH ib
1,310–1,200	Amide III (NH ib, C—N s)
1,180–850	C—C s, N—C s, CH_2 r
800–700	C=O ob, NH ob, C—N t
<700	Skeletal s, b, t

s, stretch; b, bend; w, wag; t, torsion; r, rock; i, in-plane; o, out-of-plane.
* Taken from references 1–12.

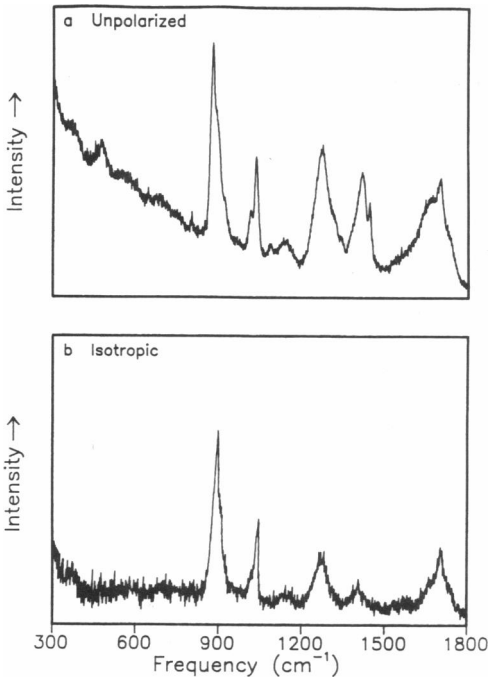

FIGURE 5 Raman spectra of glycylglycylglycine (G_3) cations in aqueous solution at room temperature: (*a*) Unpolarized; (*b*) isotropic.

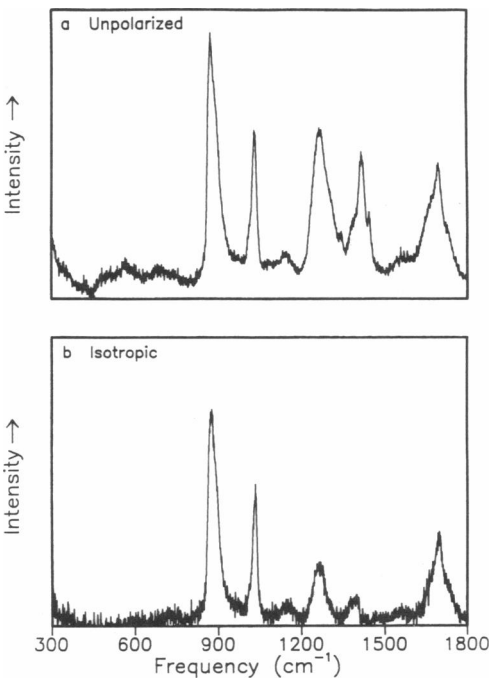

FIGURE 6 Raman spectra of glycylglycylglycylglycine (G_4) cations in aqueous solution at room temperature: (*a*) Unpolarized; (*b*) isotropic.

main features of the isotropic spectra of G_3 and G_4 are similar. In the next section, we note a similar convergence for the cation solutions and for ordered (solid state) glycine oligomers as well.

The number of bands in the region of 850–950 cm^{-1} of the isotropic Raman spectra increases systematically with the length of the disordered glycine chains. G_1 has one band in this region, G_2 two, G_3 three, and G_4 at least four. These bands, being polarized, are associated with C—C and N—C stretching modes.

Isotropic Raman spectra of the cations

The unpolarized and isotropic Raman spectra of the cations G_3 and G_4 are shown in Figs. 5 and 6, respectively; the unpolarized spectrum of G_5 is shown in Fig. 7.

There are some differences between the spectra of the cations and the corresponding zwitterions. One is that the cation spectra are significantly simpler, as is evident from a comparison of the unpolarized spectra of the G_3 and G_4 zwitterions (Figs. 3 and 4) with the corresponding spectra of the G_3 and G_4 cations (Figs. 5 and 6). The most noticeable difference in going from the zwitterion to the cation is in the reduction of intensity in the bands near 920, 1,320, and 1,395 cm^{-1}. Part of this reduction may be related to a change of the end group from COO^- to COOH.

In addition to intensity reductions in some bands in going from zwitterions to cations, there is also some band broadening. For example, the 877-cm^{-1} band, which is associated with C—C and C—N stretching modes, is broader in the cation spectra for both G_3 and G_4. This broadening, which may be associated with multiple bands, is more pronounced for the longer chains. There are other bands in the 1,100–1,000-cm^{-1} region that behave similarly to the 877-cm^{-1} band.

The isotropic Raman spectra of the glycyl peptide cations become simpler and more alike as the length of the chain increases. Such a trend has already been noted for the zwitterions. There is, however, one significant difference in this behavior for the cations and zwitterions. In the cation case, significantly fewer monomer units are required to reach what is essentially an invariant spectrum. Thus, the isotropic spectrum of the G_3 cation is not much different from that of the G_4 cation. Although the isotropic spectrum of G_5 is not available for the cat-

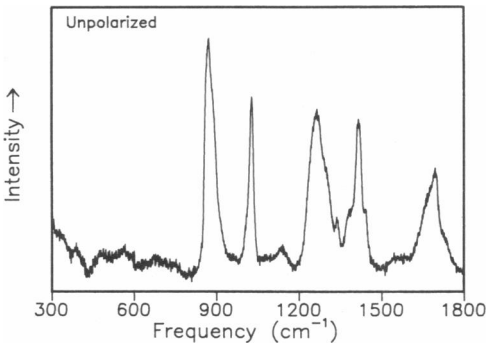

FIGURE 7 Raman spectra of glycylglycylglycylglycylglycine (G_5) cations in aqueous solution at room temperature: unpolarized.

ion, it appears that this spectrum would also conform to this trend since the unpolarized spectrum of G_5 is nearly the same as that of G_4.

CALCULATED ISOTROPIC RAMAN OF MODEL PEPTIDES

To identify the features of the isotropic Raman spectra of peptides and to characterize the general behavior of their Raman bands as a function of chain length and disorder, we have calculated Raman spectra of a series of conformationally ordered and disordered model chains that represent the peptides $CH_3CONH-(CH_2-CONH)_n-CH_3$. As noted earlier, a number of assumptions were made to simplify the calculations. Recapitulating these: the CH_2 and CH_3 groups have been condensed to single atoms; a diagonal force constant matrix was used in which the values of the force constants were selected to give the general features of polypeptide spectra; hydrogen bonding and intermolecular interactions were neglected; only isotropic polarizability derivatives for bond stretching were included; conformers were generated by randomly selecting one of the seven possible local conformations about each connecting CH_2 group. For the calculation of isotropic Raman intensity, we assumed that the value of the mean-polarizability derivative for C=O stretching was twice that for the other bonds, which tend to be single bonds. This assumption is in keeping with the finding of Yoshino and Bernstein (25) that the value of the polarizability derivative for CC bond stretching is approximately proportional to the bond multiplicity.

As a result of these approximations, the calculated spectra are only approximate representations of the observed spectra of glycyl peptides. However, the dependence of the calculated spectra on chain length and conformation closely mimics that of the observed spectra.

Ordered chains

Fig. 8 shows calculated isotropic Raman spectra of ordered all-*trans* ($\phi = \psi = 180°$) peptides of chain lengths n = 2–5, 10, and 20. As expected, the calculated spectra change as the chain length increases. These changes are most pronounced in the frequency region > 1,000 cm^{-1}.

The calculated spectra tend to converge to a spectrum that represents the spectrum of an infinitely long chain. Since the spectra of the n = 10 and n = 20 peptides are very similar, it appears that a chain of ~10 monomer units is sufficiently long to ensure that the calculated spectrum will closely resemble the limiting spectrum.

The changes in the calculated spectra with an increasing length of the ordered chain are such as to indicate the presence of LAM-1–like bands in the low-frequency region (<250 cm^{-1}). The number of bands in this region increases with chain length, and the intensity of the very lowest frequency band grows at the expense of the other

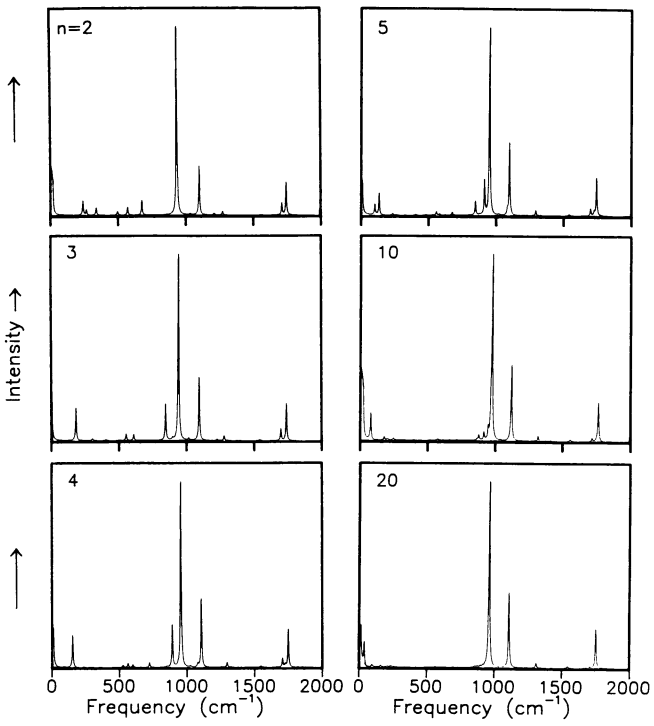

FIGURE 8 Simulated isotropic Raman spectra of all-*trans* (ordered) model peptides: (*a*) di-, (*b*) tri-, (*c*) tetra-, (*d*) penta-, (*e*) deca-, (*f*) eico-.

bands. Thus, for n = 10, only one intense band, at 61 cm^{-1}, is found. Similarly, for n = 20 a single band at 31 cm^{-1} dominates the entire region < 800 cm^{-1}. These bands are assigned to LAM-1 modes by virtue of their intensity and the fact that, as required for the LAM-*k* modes of long ordered chains (26), the value of the ratio ν/n (the frequency of the band divided by the chain length) is nearly constant. LAM-like modes also appear in the spectra of the n = 2–5 peptides but the situation for short chains is more complex because of interaction with other kinds of modes. These trends may be seen in Fig. 9 *a*, where the frequency of the most intense band in the low-frequency region of the calculated spectra is plotted against n.

We note that the basic reason for the greater complexity of the LAM-*k* modes of the polypeptides, relative to those of the *n*-alkanes, is that there are three skeletal bonds in the repeating unit of the polypeptide backbone, rather than one as is the case for the *n*-alkanes.

Systematic frequency shifts with chain length are also found for the most intense band in the 900–950-cm^{-1} region of the calculated spectra. The frequency of this band, which is associated with in-phase C—N and C—C stretching, at first increases, then levels off for n > 4 (Fig. 9 *b*).

Conformationally disordered chains

The calculated spectra of a series of disordered peptides, n = 2–5, are shown in Fig. 10. These spectra are much

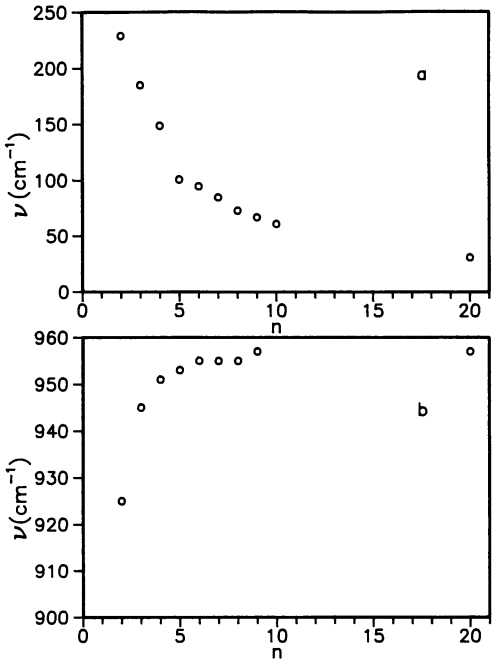

FIGURE 9 Calculated band frequencies as a function of the number of monomers for all-*trans* (ordered) model peptides: (*a*) the "LAM" bands; (*b*) skeletal stretching bands.

less chain length dependent than the corresponding spectra of the ordered peptides.

There is a significant dependence on chain length, however, in the frequency region 200–650 cm^{-1}. As chain length increases, the sharp band that occurs at ~320 cm^{-1} in the spectrum of the shortest chain ($n = 2$) becomes a multiband complex that broadens and moves to lower frequencies. This behavior is similar to that observed for the bands in the spectra of *n*-alkanes that are related to the LAM vibrations (15, 16). The band found near 580 cm^{-1} in the $n = 2$ peptide spectrum also breaks up as chain length increases. In going from the dipeptide to the tripeptide, the number of bands increases in the higher frequency region extending from 780 to 900 cm^{-1}. In going to tetra- and pentapeptides, however, no further increase in the number of bands is found, although there are band frequency shifts and bandwidth increases.

The spectra of the model of disordered peptides were also calculated as a function of sample temperature. The trends, not shown here, are those expected from changes in the conformer distribution. As temperature increases, so do the contributions from high energy conformations. The dependency on chain length becomes increasingly weaker as temperature increases.

Conformationally sensitive Raman bands

It is useful to identify bands that characterize chain disorder. The group of amide bands (amide I, amide II, etc.), which are much used to characterize the conformation of this group, are associated with localized modes, the frequencies of which are more or less dependent on the nature of the hydrogen bonding associated with local structural configuration. In contrast, the frequencies of the bands associated with delocalized modes are directly related to the conformation of the chain.

Fig. 11, which displays the calculated frequencies of Raman bands for a series of model dipeptide conformers, indicates the conformational sensitivity of these bands. Different conformers have bands that differ appreciably in frequency, and all differ from the all-*trans* form (conformer 1). In going from one conformer to another, the bands < 500 cm^{-1} vary both in frequency and in the character of their normal coordinates, in keeping with the well-known observation that low-frequency modes are in general more sensitive than high-frequency modes to conformation. It is for this reason that the low-frequency modes broaden as conformational disorder increases.

SUMMARY

The unpolarized and isotropic Raman spectra of a series of polyglycyl peptides in aqueous solution, both as zwitterions and as cations, have been measured to explore the relation between spectra and conformational disorder. The polarization measurements were exploited to verify earlier assignments and to distinguish stretching and bending bands. For some Raman bands observed in the zwitterion and cation spectra, new assignments have been suggested.

There are many similarities and differences that exist between the spectra of the zwitterions and cations. We found, for example, that the spectra of both forms of the

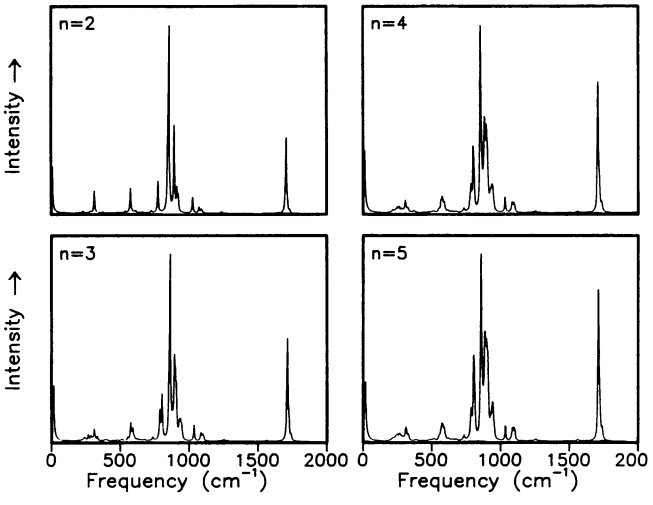

FIGURE 10 Simulated isotropic Raman spectra of conformationally disordered model peptides at 300 K: (*a*) di-, (*b*) tri-, (*c*) tetra-, and (*d*) penta-.

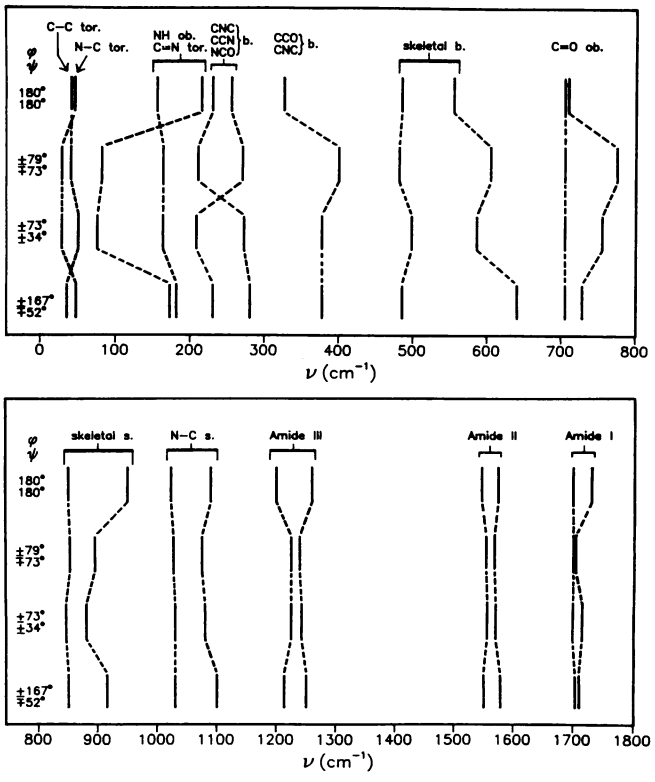

FIGURE 11 Normal frequencies for seven conformations of model dipeptides defined by the dihedral angles ϕ and ψ (see Table 1 and text). In the frequency region above 800 cm^{-1}, the character of the vibrational modes is maintained in going from one conformer to another, as indicated by the dashed lines. This is not always the case, however, in the frequency region below 800 cm^{-1} (s., stretch; b., bend; ob., out-of-plane bend; tor., torsion).

peptides change systematically with increasing chain length and converge rapidly toward the spectrum that would be associated with the infinitely long chain. The spectra of both forms also show similar kinds of multiband complexities that are attributable to conformational disorder.

There are, however, some marked differences between the spectra of the zwitterions and cations. The bands in the zwitterion spectra tend to be narrower. Consequently, the zwitterion spectra are better defined than those of the cation. This is probably attributable to the fact that there are fewer conformation possibilities for the zwitterion. The zwitterion carbonyl end-group is charged and therefore can participate in strong intramolecular interaction with other parts of the molecule through hydrogen bonding. This interaction would constrain the chain-end carbonyl group since it would promote the formation of C_7 rings (27).

Another difference between zwitterion and cation spectra is in the rate whereby the spectra simplify as the chain length is increased. The simplification occurs more rapidly for the cation. This can be attributed to the greater flexibility of the cation chain. This flexibility, the reasons for which were discussed just above, leads to a greater degree of localization of vibrational modes, so that their frequencies are less dependent on chain length.

The spectra of ordered and disordered chains differ significantly in their sensitivity to increased chain length. The spectra of disordered chains with chain lengths longer than three or four monomer units tend to be nearly alike. For conformationally ordered chains, however, chain lengths approaching at least 10 monomer units are required for comparable similarity. Since the conformers that constitute a disordered polypeptide system are in general structurally aperiodic, their vibrations tend to be more localized than the vibrations of an ordered chain. The vibrations of an ordered chain are totally delocalized. Localized modes tend to be insensitive to chain length.

The conformational disorder in the peptide chains is qualitatively manifest in the number of intense bands that is observed. This number is clearly in excess of that expected for a single conformer. Except for the very shortest peptides, the frequencies of the bands associated with the disordered chains tend to show a much weaker chain-length dependence than those in the spectrum of the ordered chain. This can be seen most clearly by comparing the calculated spectra for the ordered and disordered chains. As we have noted, the by far most prominent, chain-length dependent band is that associated with the LAM-1 mode of the ordered chains. For the disordered chains longer than the dipeptide, there are essentially no bands of appreciable chain-length dependence. However, the spectra of the disordered chains are characterized by a complex of bands, centered near 320 cm^{-1}, the center frequency of which is slightly chain-length dependent. The width of this complex increases with chain length and appears to be the polypeptide equivalent of the D-LAM band that characterizes the Raman spectra of liquid *n*-alkanes (15, 16) and other flexible chains (28).

We thank Dr. Douglas A. Cates for his help in preparing the figures.

We gratefully acknowledge the support of this research through a grant from the National Institutes of Health (GM-27690).

Received for publication 29 June 1992 and in final form 14 January 1993.

REFERENCES

1. Durig, J. R., and D. J. Gerson. 1979. *In* Infrared and Raman Spectroscopy of Biological Molecules. T. M. Theophanides, editor. Reidel, Dordrecht, Holland. 35–43.
2. Small, E. W., B. Fanconi, and W. L. Peticolas. 1970. Raman spectra and the phonon dispersion of polyglycine. *J. Chem. Phys.* 52:4369–4379.
3. Williams, R. W. 1983. Estimation of protein secondary structure from the laser Raman amide I spectrum. *J. Mol. Biol.* 166:581–603.
4. Lippert, J. L., D. Tyminsky, and P. J. Desmeules. 1976. Determi-

nation of the secondary structure of proteins by laser Raman spectroscopy. *J. Am. Chem. Soc.* 98:7075–7080.

5. Koenig, J. L. 1979. Vibrational spectroscopy of polypeptides and proteins. *In* Infrared and Raman Spectroscopy of Biological Molecules. T. M. Theophanides, editor. Reidel, Dordrecht, Holland. 109–124 (and references therein).
6. Dwivedi, A. M., and S. Krimm. 1982. Vibrational analysis of peptides, polypeptides, and proteins. X. Poly(glycine I) and its isotopic derivatives. *Macromolecules.* 15:177–185.
7. Krimm, S., and J. Bandekar. 1986. Vibrational spectroscopy and conformation of peptides, polypeptides, and proteins. *In* Advances in Protein Chemistry. C. B. Anfinsen, J. T. Edsall, and F. M. Richards, editors. Academic Press, New York. 181–364.
8. Fanconi, B. 1973. Low-frequency vibrational spectra of some homopolypeptides in the solid state. *Biopolymers.* 12:2759–2776.
9. Destrade, C., and C. Garrigon-Lagrange. 1976. Utilisation du calc des modes normaux de vibration pour la determination de la conformation de la glycylglycine et de la triglycine en solution aqueuse. *J. Mol. Struct.* 31:301–317.
10. Avignon, M., C. Garrigon-Lagrange, and P. Bothorel. 1972. Analyse conformationelle des dipeptides en solution aqueuse. I. Etude d'une serie d'amides modeles par diffusion Rayleigh depolarisée et spectroscopie Raman. *J. Chim. Phys.* 69:64–70.
11. Avignon, M., C. Garrigon-Lagrange, and P. Bothorel. 1973. Conformational analysis of dipeptides. II. Molecular structure of glycine and alanine dipeptides by depolarized Rayleigh scattering and laser Raman spectroscopy. *Biopolymers.* 12:1651–1669.
12. Peticolas, W. L. 1979. Low frequency vibrations and the dynamics of proteins and polypeptides. Methods Enzymol. 61:425–458.
13. Brooks, B., and M. Karplus. 1983. Harmonic dynamics of proteins: normal modes and fluctuations in bovine pancreatic trypsin inhibitor. *Proc. Natl. Acad. Sci. USA.* 80:6571–6575.
14. Go, N., T. Noguti, and T. Nishikawa. 1983. Dynamics of a small globular protein in terms of low-frequency vibrational modes. *Proc. Natl. Acad. Sci. USA.* 80:3696–3700.
15. Snyder, R. G. 1982. The structure of chain molecules in the liquid state: low frequency Raman spectra of *n*-alkanes and perfluoro-*n*-alkanes. *J. Chem. Phys.* 76:3921–3927.
16. Snyder, R. G., and Yesook Kim. 1991. Conformation and low-frequency isotropic Raman spectra of the liquid *n*-alkanes C_4–C_9. *J. Phys. Chem.* 95:602–610.
17. Snyder, R. G., and H. L. Strauss. 1987. Numerical studies of disordered-chain vibrations. I. Low-frequency modes of polymethylene-like skeletal chains. *J. Chem. Phys.* 87:3779–3788.
18. MacPhail, R. A., and R. G. Snyder. 1989. Torsional damping and solvent friction in liquid n-butane: experimental estimates from Raman spectroscopy. *J. Chem. Phys.* 91:3895–3902.
19. Snyder, R. G. 1992. Chain conformation from the direct calculation of the Raman spectra of the liquid *n*-alkanes C_{12}–C_{20}. *J. Chem. Soc. Faraday Trans.* 88:1823–1833.
20. Snyder, R. G. 1967. Vibrational study of the chain conformation of the liquid *n*-paraffins and molten polyethylene. *J. Chem. Phys.* 47:1316–1360.
21. Long, D. A. 1953. Intensities in Raman spectra. I. A bond polarizability theory. *Proc. R. Soc. Edinb. Sect. A Math. Phys. Sci.* 217:203–221.
22. Long, D. A., R. B. Gravenor, and D. C. Milner. 1963. Intensities in Raman spectra. Part 8. Intensity measurements in $CHCl_3$ and $CDCl_3$. *Trans. Faraday Soc.* 59:46–52.
23. Snyder, R. G. 1970. A bond polarizability interpretation of the Raman intensities of cyclohexane and cyclohexane-d_{12}. *J. Mol. Spec.* 36:204–221.
24. Vasquez, M., G. Nemethy, and H. A. Scheraga. 1983. Computed conformational states of the 20 naturally occurring amino acid residues and of the prototype residue α-aminobutyric acid. *Macromolecules.* 16:1043–1049.
25. Yoshino, T., and H. J. Bernstein. 1959. Intensity in the Raman effect: the mean polarizability derivatives of hydrocarbon molecules. *Spectrochim. Acta.* 14:127–141.
26. Mizushima, S., and T. Shimanouchi. 1949. Raman frequencies of *n*-paraffin molecules. *J. Am. Chem. Soc.* 71:1320–1324.
27. Schafer, L., C. Van Alsenoy, and J. N. Scarsdale. 1982. *Ab initio* studies of structural features not easily amenable to experiment. 23. Molecular structures and conformational analysis of the dipeptide *N*-acetyl-*N'*-methyl glycyl amide and the significance of local geometries for peptide structures. *J. Chem. Phys.* 76:1439–1444.
28. Snyder, R. G., and S. L. Wunder. 1986. Long-range conformational structure and low-frequency isotropic Raman spectra of some highly disordered chain molecules. *Macromolecules.* 19:496–498.